Meteoritics & Planetary Science 38, Nr 8, 1181–1186 (2003)
Abstract available online at http://meteoritics.org

Iron oxidation state in the Fe-rich layer and silica matrix of Libyan Desert Glass: A high-resolution XANES study

Gabriele GIULI,[1, 2*] Eleonora PARIS,[1, 2] Giovanni PRATESI,[3, 4]
Christian KOEBERL,[5] and Curzio CIPRIANI[3]

[1]Dipartimento di Scienze della Terra, Università di Camerino, Via G. III da Varano, 62032 Camerino (MC), Italy
[2]Unità Istituto Nazionale Fisica della Materia (INFM), Università di Camerino, Italy
[3]Museo di Storia Naturale, Sezione di Mineralogia e Litologia, Università di Firenze, Via G. la Pira 4, 50121 Firenze, Italy
[4]Museo di Scienze Planetarie della Provincia di Prato, Prato, Italy
[5]Department of Geological Sciences, University of Vienna, Althanstrasse 14, A-1090 Vienna, Austria
*Corresponding author. E-mail: gabriele.giuli@unicam.it

(Received 19 November 2002; revision accepted 30 April 2003)

Abstract–Libyan Desert Glass (LDG) is an enigmatic type of glass that occurs in western Egypt in the Libyan Desert. Fairly convincing evidence exists to show that it formed by impact, although the source crater is currently unknown. Some rare samples present dark-colored streaks with variable amounts of Fe, and they are supposed to contain a meteoritic component.

We have studied the iron local environment in an LDG sample by means of Fe K-edge high-resolution X-ray absorption near edge structure (XANES) spectroscopy to obtain quantitative data on the Fe oxidation state and coordination number in both the Fe-poor matrix and Fe-rich layers. The pre-edge peak of the high-resolution XANES spectra of the sample studied displays small but reproducible variations between Fe-poor matrix and Fe-rich layers, which is indicative of significant changes in the Fe oxidation state and coordination number. Comparison with previously obtained data for a very low-Fe sample shows that, while iron is virtually all trivalent and in tetrahedral coordination ($^{[4]}Fe^{3+}$) in the low-Fe sample, the sample containing the Fe-rich layers display a mixture of tetra-coordinated trivalent iron ($^{[4]}Fe^{3+}$) and penta-coordinated divalent iron ($^{[5]}Fe^{2+}$), with the Fe in the Fe-rich layer being more reduced than the matrix. From these data, we conclude the following: a) the significant differences in the Fe oxidation state between LDG and tektites, together with the wide intra-sample variations in the Fe-oxidation state, confirm that LDG is an impact glass and not a tektite-like glass; b) the higher Fe content, coupled with the more reduced state of the Fe, in the Fe-rich layers suggests that some or most of the Fe in these layers may be directly derived from the meteoritic projectile and that it is not of terrestrial origin.

INTRODUCTION

Libyan Desert Glass (LDG) is an enigmatic natural glass that is found in the Great Sand Sea in the Libyan Desert in western Egypt, near the Libyan border. Samples have been found over an area of about 6500 km^2. The glass, which is silica-rich (usually in the 96.59–99.26 wt% SiO_2 range according to Koeberl [1997]) and has very low contents of all other elements, occurs as cm- to dm-sized irregular and strongly wind-eroded pieces. Because of the low K (and, therefore, low Ar) content, ages for the LDG were measured by fission-track dating; the best results are 29.4 ± 0.5 Ma (plateau age; Storzer and Wagner 1977) and 28.5 ± 0.8 Ma (Bigazzi and De Michele 1996). The origin of LDG has been the subject of much debate with many studies supporting the opinion that LDG is an impact glass (e.g., Kleinmann 1969; Barnes and Underwood 1976; Fudali 1981). However, the lack of an evident impact crater still causes frustration. Various other suggestions for the origin of LDG were made (e.g., a sol-gel process or a sedimentary origin), but none of these suggestions are supported by any evidence. Support for an impact origin includes the presence of schlieren and partly digested mineral phases, such as lechatelierite (a high temperature melt of quartz) and baddeleyite, a high temperature break-down product of zircon (for recent summaries of the evidence, see, e.g., Horn et al. [1997] and Koeberl [1997]). The source material of the glass remains a mystery. Storzer and Koeberl (1991) suggested from their Zr/

© Meteoritical Society, 2003. Printed in USA.

U and REE data that none of the sands or sandstones from various sources are good candidates to be the sole precursors of LDG. Compositional data for surface sands (Koeberl 1997) show significant differences to the average LDG composition. Some chemical and isotopic similarity exists between rocks from the BP and Oasis impact structures in Libya (Abate et al. 1999), which are at a distance of about 150 km from the LDG area but are of unknown age; in addition, a recent detailed isotopic analysis of LDG in the Rb-Sr and Sm-Nd systems (Schaaf and Müller-Sohnius 2002) suggests that Nubian Group rocks (such as those exposed at BP and Oasis) are not likely precursors of LDG. To complicate things even further, Barakat (2001) and Kleinmann et al. (2001) found some shocked quartz-bearing breccias in the LDG strewn field, but, so far, no evidence for a crater.

More importantly, though, is the existence of a meteoritic component in LDG (Murali et al. 1997; Rocchia et al. 1996; Koeberl 1997). These authors have found that the contents of siderophile elements, such as Co, Ni, and Ir, are significantly enriched in some rare, dark bands that occur in some LDG samples. Koeberl (1997) studied such dark bands and found that the contents of Fe, Mg, and Ni are high in the dark zones and low in the "normal" LDG. This co-variation can only be explained by a common source for those elements. Together with the observations of Murali et al. (1997), Rocchia et al. (1996), and Koeberl (1997) of high Ir contents in the dark zones, these data are only consistent with the presence of a meteoritic component. This is also in agreement with Os isotopic data of dark bands in LDG (Koeberl 2000). TEM investigation of the dark streaks (Pratesi et al. 2002) also revealed the presence of small (about 100 nm) amorphous Fe-rich silicate spherules, within the silica-glass matrix, resulting from silicate-silicate liquid immiscibility.

In the present study, we attempt to characterize the Fe oxidation state and coordination number in LDG to test if a difference for these parameters exists between the Fe-poor matrix and the Fe-rich dark bands that could be the result of meteoritic contamination. X-ray absorption spectroscopy (XAS) is used as a method that allows structural and chemical determinations and has the advantage over other spectroscopic techniques of also being used to study very diluted elements or complex chemical systems. The information obtained by XAS on the glasses are compared with those available for well-characterized model compounds. High resolution XANES spectra have been found to give structural data on the local geometry around the selected element and a quantitative evaluation of the different oxidation states (Wilke et al. 2001).

SAMPLES AND EXPERIMENTAL METHODS

Two samples were chosen from those available so as to span a relatively wide range in Fe-content (see Table 1). One sample was taken to be representative of "normal" LDG, i.e., a greenish-yellow, slightly turbid glass without any unusually colored bands. This sample, from the collections of the Museo di Storia Naturale of the Università di Firenze (catalogue number RI2670), was described before (e.g., Giuli et al. 2002). A second sample, with the dark brown layer, is a piece of Libyan Desert Glass from the collection of the Institute of Geochemistry (catalog number LDG-98/01), University of Vienna. It is a fragment of a larger piece described by Koeberl (1997).

Table 1. Average major elements composition.[a]

	RI2670	LDG-98/01 matrix	LDG-98/01 dark streak
SiO_2	98.44 (29)	98.27 (29)	95.85 (28)
Al_2O_3	0.55 (0)	1.30 (2)	1.48 (3)
Cr_2O_3	<0.01	0.01 (0)	0.03 (1)
FeO	0.09 (3)	0.12 (3)	0.98 (6)
MnO	<0.01	<0.01	0.02 (1)
CaO	<0.01	0.01 (0)	0.08 (1)
MgO	<0.01	0.01 (0)	1.38 (2)
K_2O	0.01 (0)	0.01 (0)	0.01 (0)
Na_2O	0.01 (0)	0.03 (1)	0.02 (1)
TiO_2	0.08 (2)	0.17 (2)	0.18 (2)
P_2O_5	<0.01	<0.01	<0.01
Total	99.18	99.93	100.03

[a](Oxide wt%); uncertainties in the last decimal place are shown in parentheses.

Chemical compositions were obtained by means of a JEOL JXA 8600 electron microprobe operating at 15.0 kV and 10.0 nA and with the electron beam defocused to a radius of 20 μm. The standards used are: albite for Si and Na, anorthite for Al, ilmenite for Fe and Ti, chromite for Cr, bustamite for Mn, diopside for Ca, olivine for Mg, and sanidine for K. Data were corrected according to the method of Bence and Albee (1968). Tabulated data are averages of 7 individual analyses (Table 1).

The standards used for XAS measurements are a staurolite from Canton Ticino (Switzerland) and a synthetic Fe-akermanite for Fe^{2+} in tetrahedral coordination, a grandidierite from Madagascar for Fe^{2+} in trigonal dipyramidal coordination, a synthetic kirschsteinite and a siderite from Erzberg (Austria) for Fe^{2+} in octahedral coordination, a natural andradite for Fe^{3+} in octahedral coordination, and a natural yoderite from Mautia Hills (Tanzania) for Fe^{3+} in 5-fold coordination. The natural standards were separated by hand picking from thumb-sized crystals choosing the clearest portions to avoid impurities. All the standards were checked for purity by both optical microscopy and X-ray diffraction.

Samples for XAS measurement were prepared by smearing finely ground powder on a kapton tape, while the LDG sample with Fe-rich layers consisted of a blocky piece of glass with a flat surface cut perpendicularly to the layers; the flat surface was placed at 45° from the X-ray beam directed toward the fluorescence detector. High resolution XANES spectra were collected at the beamline BM-8 of the

ESRF (European Synchrotron Radiation Facility) storage ring (Grenoble, France) operating at 6 GeV and with the ring current ranging from 150 to 200 mA. Radiation was monochromatized by means of 2 channel-cut Si (311) crystals. Spectra were recorded in step-scan mode measuring the incident beam intensity with an ionization chamber and the fluorescence yield with a high purity Ge detector. Scans ranged from 7000 eV to 7300 eV with 0.2 eV steps and 8 sec counting times. While the configuration of the optical elements (mirrors, slits, etc.) was maintained constant so as to have comparable resolution for all the spectra (~0.2 eV), the size of the beam at the sample was varied by adjusting a window just before the sample to have comparable counting statistics for both samples and standards, thus avoiding problems related to detector saturation. The area sampled by the X-ray beam on the LDG samples was about 10 × 1 mm.

DATA REDUCTION

Experimental XANES spectra were reduced by background subtraction with a linear function and then normalized for atomic absorption on the average absorption coefficient of the spectral region from 7150 to 7300 eV. The energy was calibrated against a standard of Fe metal (7112 eV). The threshold energy was taken as the first maximum of the first derivative of the spectra, while peak positions were obtained by calculating the second derivative of the spectra. Pre-edge peak analysis was carried out following the same procedure reported in Wilke et al. (2001) and Giuli et al. (2002). The pre-edge peak was fitted by a sum of pseudo-Voigt functions, and the integrated intensities along with centroid energies were compared with those of the standards analyzed here and others from the literature (Wilke et al. 2001; Farges 2001[1]) to extract information on Fe oxidation state and coordination number in the glasses studied.

RESULTS

XANES spectra of the Fe model compounds are shown in Fig. 1a, whereas those of the LDG samples are shown in Fig 1b. The XANES spectra of the LDG samples are less structured than those of the standards because of the amorphous nature of the former producing absence of a long-range order. Apart from the different overall shape, which is due to the different structure of the model compounds, clear differences can be noted in the energy region before 7120 eV, called the pre-edge region. The peak located in the pre-edge region (the pre-edge peak) is the most useful feature to discriminate the oxidation state and coordination number of Fe (Fig. 2). This peak represents an s-d-like transition and is, thus, dipole-forbidden, but it becomes partially allowed by mixing the d-states of the transition metal with the p-states of the surrounding oxygen atoms. Its energy position depends

[1]As Wilke et al. (2001) and Farges (2001) calibrated the edge energy of Fe metal at 7111.08 eV, their values have been rescaled accordingly to be compared to our values. On the whole, a good agreement exists in both energy and intensity in the 3 sets of standards.

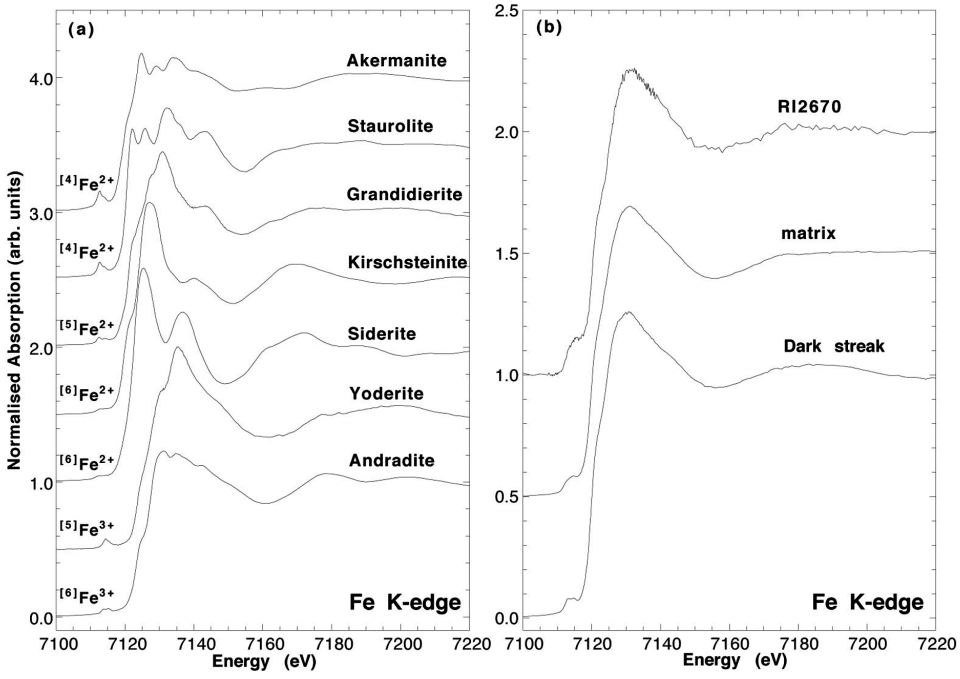

Fig. 1. Experimental Fe K-edge XANES spectra of: a) model compounds with Fe in different oxidation states and coordination numbers; b) Libyan Desert Glass samples. The spectra have been normalized by setting the step height to 1.

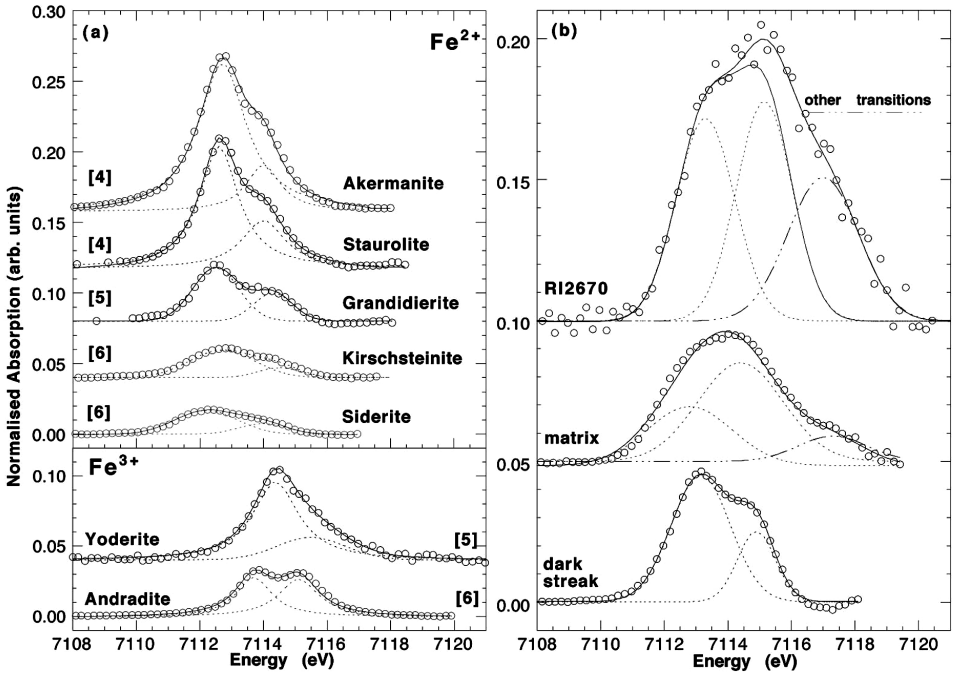

Fig. 2. Fit of the pre-edge peak of: a) model compounds with Fe in different oxidation states and co-ordination numbers; b) Libyan Desert Glass samples. The energy scale in the (b) panel has been modified in order to accommodate the pre-edge peak of the LDG sample.

mainly on the mean Fe oxidation state, gradually increasing from Fe^{2+} to Fe^{3+}, while its intensity depends on the geometry around Fe (Calas and Petiau 1983; Brown et al. 1995; Wilke et al. 2001). The intensity will be virtually zero in the case of regular octahedral symmetry (O_h) around the absorber, while it will reach its maximum in the case of tetrahedral coordination (T_d). For these characteristics of the XANES spectra, we analyzed model compounds chosen to represent a variety of oxidation states (from Fe^{2+} to Fe^{3+}) and coordination numbers (from 4 to 6). Fig. 2 shows in detail how the pre-edge peak varies as a function of these parameters both in the model compounds and in the LDG samples, also indicating the results of the pre-edge peak's deconvolution into single components.

Note in Fig. 2b that the pre-edge peak of the LDG XANES spectra undergoes dramatic changes when passing from the Fe-poor sample (RI2670) to the sample with dark streaks. Moreover, even within the latter sample, clear variations related to the shape of the pre-edge peak exist. These changes are made more evident when considering the centroid energy and integrated intensity. To extract as much quantitative information as possible from the pre-edge peaks, their integrated intensity is plotted versus the energy position of their centroids in Fig. 3 (Table 2), along with those of the standards used in this study and the data reported in Wilke et al. (2001) and Farges (2001).

The pre-edge peak of the matrix spectrum is shifted at higher energy by ~0.3 eV with respect to that of the dark streak spectrum; moreover, the pre-edge peak of the matrix spectrum has a slightly higher integrated intensity. Both these changes are well reproducible as the values reported were consistently found to be constant for all the spectra recorded for the Fe-rich layer and the matrix (2 and 3 different spectra, respectively). So, although the accuracy of the reported energy is about 0.1 eV, the precision is close to 0.05 eV. Keeping this in mind, we must remark that, while the absolute energy position of the 2 pre-edge peaks has an accuracy of 0.1 eV, the difference in energy between the 2 peaks (and, thus, the variation in the Fe oxidation state) is real and significant.

Table 2. Pre-edge peak features of the Fe K-edge XANES spectra.

Sample name	Centroid (eV)[a]	Integrated intensity	Fit agreement index (%)
Siderite	7112.8	0.054	99.84
Kirschsteinite	7113.0	0.062	99.83
Grandidierite	7113.0	0.101	99.32
Staurolite	7113.0	0.218	99.88
Fe-Akermanite	7112.9	0.283	99.84
Andradite	7114.4	0.107	99.93
Yoderite	7114.3	0.169	99.91
RI2670	7114.2	0.333	99.42
LDG-98/01[b]	7113.6	0.147	99.81
LDG-98/01[c]	7113.9	0.193	99.79

[a]Precision and accuracy of the pre-edge peak centroid energy are ±0.05 and 0.1 eV, respectively.
[b]Dark streak.
[c]Fe-poor matrix.

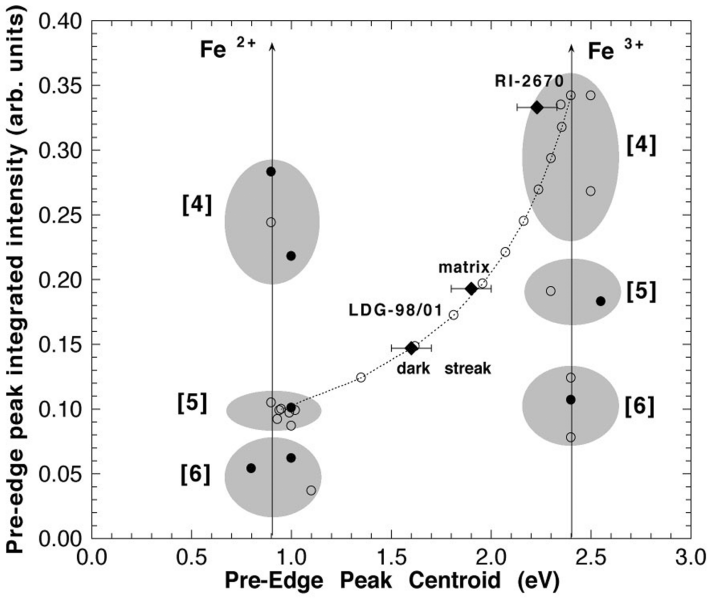

Fig. 3. Plot of the pre-edge peak integrated intensity versus centroid energy. The solid symbols refer to the samples studied here (diamond = Libyan Desert Glass, small circles = model compounds), while the empty symbols refer to the Fe model compounds reported in Wilke et al. (2001) and Farges (2001). The zero-energy refers to the edge energy of metallic Fe. The mixing line (dashed line + circles) between $^{[5]}Fe^{2+}$ and $^{[4]}Fe^{3+}$ is also shown (see text).

The energy position of the pre-edge peaks is intermediate between those of Fe^{2+} and Fe^{3+} model compounds, indicating the presence of both Fe oxidation states in the samples examined; moreover, the slightly higher energy of the centroid of the matrix spectrum indicates Fe to be more oxidized in the matrix relative to the dark streak. To estimate the amount of divalent versus trivalent Fe, the pre-edge peaks of the Fe model compounds have been summed with different weights according to the procedure of Wilke et al. (2001). As seen in Fig. 3 and in the results of Wilke et al. (2001), the energy and intensity of the pre-edge peak gradually increase in passing from the purely divalent to the purely trivalent oxidation state. In particular, as noted by Wilke et al. (2001), the change in energy and intensity is not linearly related to the mean Fe oxidation state so that one must take both the integrated intensity and the centroid energy into consideration when trying to estimate the contribution of divalent and trivalent Fe. In our case, the position of the spectral features of the pre-edge peaks is compatible with different possibilities in terms of oxidation states and coordination numbers: while the sample RI2670 can be interpreted as containing almost solely tetra-coordinated trivalent iron ($^{[4]}Fe^{3+}$), the data for the matrix and dark streak of the LDG-98/01 sample can be interpreted in two ways. The matrix can be interpreted either as a mixture of $^{[5]}Fe^{2+}$ and $^{[4]}Fe^{3+}$ or as a mixture of $^{[4]}Fe^{2+}$ and $^{[5]}Fe^{3+}$, while the dark streak can be interpreted either as a mixture of $^{[4]}Fe^{2+}$ and $^{[6]}Fe^{3+}$ or as a mixture of $^{[5]}Fe^{2+}$ and $^{[4]}Fe^{3+}$. However, considering the data for the (Fe-poor) LDG sample (Giuli et al. 2002) revealing the presence of $^{[4]}Fe^{3+}$ and keeping in mind that, more commonly, Fe in natural glasses has been found to be $^{[5]}Fe^{2+}$ and $^{[4]}Fe^{3+}$ (Galoisy and Calas 2001), all LDG samples examined seem more likely to plot on the same mixing line between $^{[5]}Fe^{2+}$ and $^{[4]}Fe^{3+}$, as shown in Fig. 3. A quantitative evaluation using the mixing curve shows that, in the case of the LDG sample with the Fe-rich layers, the Fe in the Fe-rich dark bands would consist of about 80% $^{[5]}Fe^{2+}$ and 20% $^{[4]}Fe^{3+}$, while the Fe-poor matrix consists of about 63% $^{[5]}Fe^{2+}$ and 37% $^{[4]}Fe^{3+}$.

DISCUSSION AND CONCLUSIONS

Our data show that a significant and reproducible difference in Fe oxidation state and coordination number exists between the Fe-rich dark bands and the Fe-poor matrix of Libyan Desert Glass. Comparing the results for LDG with those of other impact-derived glasses, namely tektites and impact glasses, some interesting observations can be made. Iron in tektites (distal glassy ejecta from geographically extended strewn fields) occurs predominantly as Fe^{2+}, more precisely, a mixture of 4- and 5-fold coordinated iron ($^{[4]}Fe^{2+}$ and $^{[5]}Fe^{2+}$), while Fe in impact glasses (proximal glassy ejecta found at specific impact craters) can span a much wider range in Fe oxidation states (from purely divalent to purely trivalent), comprising mixtures of various coordination numbers (Rossano et al. 1999; Giuli et al. 2002). In natural sediments (such as those that make up typical crustal target rocks), Fe is often reported to be predominantly trivalent (see, e.g., Blatt et al. 1980), although in a small number of sedimentary settings, Fe can also be in divalent form.

The XANES data for the Fe-poor matrix and the Fe-rich

layer in a LDG sample, along with data for a "normal" (even more Fe-poor) sample of LDG (Giuli et al. 2002), can all be explained in terms of different mixtures of $^{[5]}Fe^{2+}$ and $^{[4]}Fe^{3+}$. The Fe content between the "normal" LDG sample and the sample with the Fe-rich layers is different by more than a factor of 10. The data point for the very low Fe sample plots directly within the $^{[4]}Fe^{3+}$ field (Fig. 3), while the Fe in the matrix of the sample with the layers, which has a higher Fe content than the "normal" sample, is a mixture of $^{[5]}Fe^{2+}$ and $^{[4]}Fe^{3+}$. These data show that LDG is quite different from tektites. Furthermore, Fe in the dark layers is less oxidized than Fe in the corresponding matrix. As abundant evidence (from platinum group element patterns and Os isotopes; e.g., Rocchia et al. 1996; Koeberl 2000) shows that the dark layers contain a significant meteoritic component, Fe, too, is likely to be mostly of extraterrestrial origin. Even though the possibility exists of some Fe being of terrestrial origin, given the association with other meteoritic traces, meteoritic iron, which has not been completely mixed with terrestrial iron, more likely predominates.

Acknowledgments–We wish to thank the staff of beamline BM-08 (ESRF) for assistance during the XAS measurements. F. Seifert and V. Schenk kindly provided the synthetic Fe-akermanite and natural yoderite, respectively. The synthetic kirschsteinite was done at the Bayerisches Geoinstitut (Bayreuth) thanks to the EC "Human Capital and Mobility—Access to Large Scale Facility" program (contract no. ERBCHGECT940053 to D. C. Rubie). C. Koeberl is supported by the Austrian Science Foundation (grant Y58-GEO). Grants from CNR and MIUR to E. Paris are acknowledged. Useful suggestions by M. Wilke and M. Zolensky were greatly appreciated.

Editorial Handling—Dr. Urs Krähenbühl

REFERENCES

Abate B., Koeberl C., Kruger F. J., and Underwood J. R., Jr. 1999. BP and oasis impact structures, Libya, and their relation to Libyan Desert Glass. In *Large meteorite impacts and planetary evolution II,* edited by Dressler B. O. and Sharpton V. L. Boulder: Geological Society of America. Special Paper 339. pp. 177–192.

Barakat A. A. 2001. Hypervelocity meteorite impact features within the Libyan Glass area. *Annals of the Geological Survey of Egypt* 5:24.

Barnes V. E. and Underwood J. R., Jr. 1976. New investigations of the strewn field of Libyan Desert Glass and its petrography. *Earth and Planetary Science Letters* 30:117–122.

Bence A. E. and Albee A. L. 1968. Empirical correction factors for the electron microanalysis of silicates and oxides. *The Journal of Geology* 76:382–402.

Bigazzi G. and De Michele V. 1996. New fission-track age determinations on impact glasses. *Meteoritics & Planetary Science* 31:234–236.

Blatt H., Middleton G., and Murray R. 1980. Origin of sedimentary rocks. Englewood Cliffs: Prentice-Hall. 776 p.

Brown G. E., Farges F., and Calas G. 1995. X-ray scattering and X-ray spectroscopy studies of silicate melts. In *Structure, dynamics and properties of silicate melts,* edited by Stebbins J. F., McMillan P. F., and Dingwell D. Washington D.C.: Mineralogical Society of America. pp. 317–410.

Calas G. and Petiau J. 1983. Coordination of iron in oxide glasses through high-resolution K-edge spectra: Information from the pre-edge. *Solid State Communications* 48:625–629.

Farges F. 2001. Crystal-chemistry of Fe in natural grandidierites: A XAFS spectroscopy study at the Fe K-edge. *Physics and Chemistry of Minerals* 28:619–629.

Fudali R. F. 1981. The major element chemistry of Libyan Desert Glass and the mineralogy of its precursor. *Meteoritics* 16:247–259.

Galoisy L. and Calas G. 2001. High resolution XANES spectra of iron in minerals and glasses. *Chemical Geology* 174:307–319.

Giuli G., Pratesi G., Paris E., and Cipriani C. 2002. Iron local structure in tektites and impact glasses by EXAFS and high-resolution XANES spectroscopy. *Geochimica et Cosmochimica Acta* 66: 4347–4353.

Horn P., Müller-Sohnius D., Schaaf P., Kleinmann B., and Storzer D. 1997. Potassium-argon and fission-track dating of Libyan Desert Glass, and strontium and neodymium isotope constraints in its source rocks. In *Proceedings of the Silica '96 Meeting,* edited by De Michele V. Milan: Pyramids. pp. 59–76.

Kleinmann B. 1969. The breakdown of zircon observed in the Libyan Desert Glass as evidence of its impact origin. *Earth and Planetary Science Letters* 5:497–501.

Kleinmann B., Horn P., and Langenhorst F. 2001. Evidence for shock metamorphism in sandstones from the Libyan Desert Glass strewn field. *Meteoritics & Planetary Science* 36:1277–1281.

Koeberl C. 1997. Libyan Desert Glass: Geochemical composition and origin. In *Proceedings of the Silica '96 Meeting,* edited by De Michele V. Milan: Pyramids. pp. 121–131.

Koeberl C. 2000. Confirmation of a meteoritic component in Libyan Desert Glass from osmium isotopic data (abstract). *Meteoritics & Planetary Science* 35:A89–A90.

Murali A. V., Zolensky M. E., Underwood J. R., Jr., and Giegengack R. F. 1997. Chondritic debris in Libyan Desert Glass. In *Proceedings, Silica 96, Meeting,* edited by De Michele V. Milan: Pyramids. pp. 133–142.

Pratesi G., Viti C., Cipriani C., and Mellini M. 2002. Silicate-Silicate liquid immiscibility and graphite ribbons in Libyan desert glass. *Geochimica et Cosmochimica Acta* 66:903–911.

Rocchia R., Robin E., Fröhlich F., Meon H., Frogent L., and Diemer E. 1996. L'origine des verres du désert libyque: Un impact météorique. *Comptes Rendus de l'Académie des Sciences* 322: 839–845.

Rossano S., Balan E., Morin G., Bauer J. P., Calas G., and Brouder C. 1999. ^{57}Fe Mössbauer spectroscopy of tektites. *Physics and Chemistry of Minerals* 26:530–538.

Schaaf P. and Müller-Sohnius D. 2002. Strontium and neodymium isotopic study of Libyan Desert Glass: Inherited Pan-African age signatures and new evidence for target material. *Meteoritics & Planetary Science* 37:565–576.

Storzer D. and Koeberl C. 1991. Uranium and zirconium enrichments in Libyan Desert Glass (abstract). 22nd Lunar and Planetary Science Conference. pp. 1345–1346.

Storzer D. and Wagner G. A. 1977. Fission track dating of meteorite impacts (abstract). *Meteoritics* 12:368–369.

Wilke M., Farges F., Petit P. E., Brown G. E., and Martin F. 2001. Oxidation state and coordination of Fe in minerals: An Fe K-XANES spectroscopic study. *American Mineralogist* 86:714–730.